
BatchGNN: Efficient CPU-Based Distributed GNN Training on Very Large Graphs

Loc Hoang
KatanaGraph
loc@katanagraph.com

Rita Brugarolas Brufau
Intel Corporation
rita.brugarolas.brufau@intel.com

Ke Ding
Intel Corporation
ke.ding@intel.com

Bo Wu
Colorado School of Mines *
bwu@mines.edu

Abstract

We present BatchGNN, a distributed CPU system that showcases techniques that can be used to efficiently train GNNs on terabyte-sized graphs. It reduces communication overhead with *macrobatching* in which multiple minibatches' subgraph sampling and feature fetching are batched into one communication relay to reduce redundant feature fetches when input features are static. BatchGNN provides integrated graph partitioning and native GNN layer implementations to improve runtime, and it can cache aggregated input features to further reduce sampling overhead. BatchGNN achieves an average $3\times$ speedup over DistDGL on three GNN models trained on OGBN graphs, outperforms the runtimes reported by distributed GPU systems P³ and DistDGLv2, and scales to a terabyte-sized graph.

1 Introduction

Graph neural networks (GNNs) apply machine learning onto graphs by generating or transforming features on vertices and edges using deep neural networks. Once a GNN model is trained, it can be used in areas like fraud detection with node classification [6], product relationship prediction [1] with link prediction, and drug discovery using GNN-based graph generation [4].

Training GNNs on large graphs is compute intensive. In addition, real-world graphs like social networks or purchase graphs easily reach terabyte scale as they can contain billions of vertices and trillions of edges. To reduce computational and memory costs of GNN training, many GNN systems consider a sample of neighbors in a minibatch (a batch of training vertices instead of all vertices) to reduce the memory and computational load. Many systems adopt this execution model because it has been observed to have a positive effect on training [19, 36] and because the smaller memory footprint allows the use of GPUs which have limited memory compared to CPUs.

Distributed CPU/GPU GNN systems like P³ [9] and DistDGL [35] provide increased computational power and more memory in addition to providing sampling and minibatching to efficiently train larger graphs. These systems vary in the assumptions they make: some assume there is enough memory to fit the entire graph on each machine while others *partition* the graph among machines. SALIENT [17] and PyTorch Geometric [7] fall into the first category and can only handle small to medium-sized graphs. Systems like DistGNN [22] and DistDGL [35] are part of the second category, and this is the approach this paper focuses on since it allows training of arbitrarily large graphs via scale-out. One problem with this approach is that the communication overhead during training can be high. Unless

*Bo Wu contributed to this work while employed at KatanaGraph.

the full computational subgraph exists locally or is fetched before training, an updated vertex feature must be communicated to all machines that need a copy of it. There are techniques to reduce the overhead of this communication by allowing stale features or approximating features [8, 22, 28], but they change the semantics of training. Alternatively, some systems fetch the entire computational subgraph to a local machine before training. This requires topology fetching and initial feature fetching, but no communication occurs during training aside from gradient updates.

Existing distributed GNN systems are typically bottlenecked by the communication required to do training. For example, in P³ [9], every machine sends a local minibatched subgraph to all other machines for computation (because the features are divided among all machines), and the final hidden features are reduced from all machines. This approach fails to scale: it is slower than DistDGL if the hidden feature size of the GNN is sufficiently large [9] because hidden features are communicated, and more machines means more communication partners for all processes. DistDGL, on the other hand, suffers from excessive redundant features fetches. In 1 epoch for a 3-layer GNN using a minibatch size 1024 on various Open Graph Benchmark (OGB) [14] graphs, the number of fetched features can be more than ten times larger than the number of vertices of the graph (Table 5 in Section 4). Sampling bottlenecks extend to GPU GNN systems as well. Distributed sampling typically occurs on CPUs, so GPU systems have the same sampling overheads as CPU systems in addition the copy cost of sampled subgraphs from CPU to GPUs. Even if all stages of training executed on GPUs, such a system would demand a larger number of GPUs than CPUs since GPUs have less memory than CPUs which could lead to a more expensive cluster than a CPU cluster.

We address these problems in BatchGNN, a distributed end-to-end GNN training system on CPUs. We use a sampling scheme called *macrobatching* which *batches the minibatches* and communicates subgraphs and vertex features for M minibatches in one communication relay rather than M relays when the features do not change during training. This reduces redundant feature fetching by doing it for M minibatches at once. BatchGNN accelerates end-to-end execution with an integrated distributed streaming graph partitioner and native GNN layer implementations that avoid dynamic memory allocation. BatchGNN also implements an *aggregation cache* that pre-computes the aggregation of static input features which can be fetched in lieu of doing sampling and initial feature fetching for the first GNN layer’s subgraph to reduce the overhead of sampling further.

We compare BatchGNN against DistDGL (Section 4) using GraphSAGE [11], Graph Convolutional Network (GCN) [20], and Graph Isomorphism Network (GIN) [31] models on OGBN [14] graphs and show that it is $3\times$ faster on average than DistDGL on CPUs. By replicating the experiments conducted by state-of-the-art GPU GNN systems P³ and DistDGLv2 [36], we also show that BatchGNN is able to outperform the reported runtimes of those two GPU systems with only CPUs.

This paper makes the following major contributions:

- Presents a distributed CPU-based GNN system, BatchGNN
- Proposes *macrobatching* to lower communication overhead of minibatch subgraph sampling by reducing communication relays and redundant feature fetching
- Proposes memory-related optimizations to GNN layers and an input feature aggregation cache to elide computation for the first computational GNN layer
- Shows that BatchGNN outperforms DistDGL CPU training by $3\times$, outperforms reported performance of GPU systems P³ and DistDGLv2, and trains a terabyte scale graph

2 Background, Related Work, and Motivation

2.1 Graph Neural Networks

Graph neural networks are an application of neural networks on the features of vertices (or edges) of a graph. Formally, given a graph G with vertices V and edges E , input feature h_v^0 for vertex v , an l -layer GNN transforms h_v^0 into h_v^l through l layers of *aggregation* and *update*. The feature h_v^k after computational layer k is defined as follows:

$$a_v^k = \text{aggregate}(\{h_u^{k-1} | u \in \mathcal{N}(v)\}), \quad h_v^k = \text{update}(h_v^{k-1}, a_v^k) \tag{1}$$

Aggregation occurs over a *neighborhood* \mathcal{N} of v to get the aggregated feature, and the aggregated and original features are passed into an update function. Both steps can be parameterized. These parameters can be *trained* via supervised learning with ground truth output for a particular input. Many GNN architectures exist that differ in neighborhood definition, aggregation function, and update function such as GCN [20], GraphSAGE [11], GAT [27], and GIN [31].

2.2 GNN Systems

GNN systems facilitate the definition and training of GNNs. For example, PyTorch Geometric (PyG) [7] and DGL [29] provide graph representations and predefined GNN layers on top of PyTorch [25], a neural network learning framework, to execute on CPUs and GPUs. To reduce the cost of training, GNN systems implement *minibatching* and *sampling*. *Minibatching* processes the training set in smaller minibatches instead of all at once. This can reduce the memory footprint significantly since training on a vertex may involve a large l -hop-induced subgraph for an l -layer GNN. *Sampling* reduces the size of the l -hop-induced subgraph by sampling a fixed number of neighbors. Different methods of sampling exist such as GraphSAGE [11], GraphSAINT [33], FastGCN [5], layer-dependent importance sampling (LADIES) [37], and influence-based minibatching [10].

Large graphs may not fit on a single machine for training. Distributed GNN systems (the focus of this paper) allow training large graphs by using multiple CPU and/or GPUs in parallel for additional computational power and aggregate memory. This facilitates training on large graphs that would be infeasible to train on a single machine. Existing distributed GNN systems include Graph-Learn [32], DistDGL [35, 36], CAGNET [26], DeepGalois [12], SALIENT [17], DistGNN [22], Roc [16], GraphScope [30], Euler [2], ByteGNN [34], NeuGraph [21], and P³ [9]. Out-of-core GNN systems also allow training large graphs by reading data from disk on demand. They optimize disk reads for performance: Ginex [24], for example, determines an optimal disk read order by sampling multiple minibatches at once in a “superbatch” to determine used features in training².

2.3 Distributed GNN Training

Distributed GNN training requires graph partitioning and distributed data fetching.

Graph Partitioning Partitioning assigns the vertices and edges of a graph uniquely among all machines. Most distributed GNN systems use an edge-cut where all outgoing (or incoming) edges of a vertex get assigned to the machine that owns that vertex. This simplifies sampling since it guarantees that the owner of a vertex has all of its edges. The partitioning of vertices determines the pattern of communication for sampling and property fetching, so optimizing it is important for performance. For instance, DistDGL [35] uses METIS [18] to reduce the number of edges cut (i.e., edges with an endpoint owned by another partition) among partitions to reduce sampling/property fetching communication. Some systems like SALIENT [17] avoid partitioning by loading the entire graph on every machine. This allows the system avoid communication of topology/feature data.

Topology Sampling and Property Fetching Subgraph sampling and feature fetching require communication with other partitions. Each machine constructs a minibatch subgraph that it independently trains, and the gradients from training are reduced among machines to update the model. An alternative approach is for all machines to collectively work on the same logical subgraph rather than each sample their own subgraph (e.g., used by DistGNN [22], DeepGalois [12], and BNS-GCN [28]). These systems communicate updated vertices’ feature vectors if the updated feature is not computed locally. This does not scale because it occurs at every GNN layer unless stale values are allowed by the system. Another approach used by P³ is to communicate the “task” rather than the data. Because P³ partitions all features among all machines, each machine communicates its local subgraph to all other machines so that the other machines apply their owned features to the subgraphs. This also does not scale and is slower than DistDGL [9] for non-trivial hidden feature sizes as it requires all-to-all communication of subgraphs and the communication of computed hidden features. This paper focuses on the approach in which each machine constructs an independent subgraph.

²The high-level idea (sampling many batches at once) is similar to our proposed macrobatch technique; we use it to reduce communication. We were not aware of superbatching when we developed our technique.

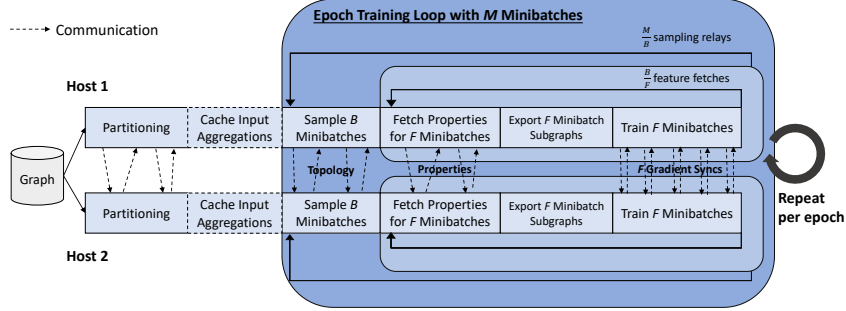


Figure 1: BatchGNN execution overview. B is the number of minibatches to sample at once and F is the number of minibatches to fetch properties for at once.

2.4 Distributed Sampling Bottlenecks

We note the following bottlenecks in distributed sampling.

High number of communication rounds for sampling Subgraph sampling requires fetching of topology from other machines with a back-and-forth communication relay that requires many rounds of waiting on request fulfillment. Lowering the number of these relays is crucial for performance.

Redundant feature fetching Redundant communication of vertex feature vectors can occur over many minibatches. For example, if a vertex A 's feature is fetched in minibatch 1 and also needs to be fetched in minibatch 2, A is redundantly fetched in minibatch 2. The possible magnitude of redundancy is shown in Table 5 where DistDGL fetches more remote features in a single epoch than the number of features that would exist if the graph was replicated on all machines.

3 BatchGNN Overview

BatchGNN is an end-to-end distributed GNN system that uses *macrobatch sampling* to reduce communication overhead. In addition, it provides integrated streaming partitioning and a subgraph exporter that allows execution with DGL, PyG, or a set of native BatchGNN GNN layers that are integrated into PyTorch's Autograd system. It also provides an input feature aggregation cache to elide the first computational layer's sampling and feature fetching. The core implementation is built on top of the Galois [23] C++ parallel library which provides graph data structures and parallel loops. Native BatchGNN GNN layers use Intel MKL [15] for matrix operations. Each machine trains on an independent sampled minibatch subgraph, and the gradients from each minibatch are synchronized via Torch Distributed Data Parallel. Figure 1 shows the flow of BatchGNN which is detailed below.

Streaming Partitioner BatchGNN's partitioner builds upon the Customizable Streaming Partitioner (CuSP) [13]. As a *streaming* partitioner, owner assignments of vertices/edges are made once and not refined unlike what an offline partitioner like METIS [18] does. Partitioning occurs on-demand in a distributed fashion for however many processes exist, and partitions do not need to be saved to disk (but it is possible to do). Because partitioning is on-demand, the user does not need to run an offline partitioner for every rank count configuration (e.g., DistDGL requires offline partitioning for each number of ranks). BatchGNN uses edge-cut partitions to facilitate fast topology sampling during training (see Section 2.3). BatchGNN also adds efficient feature vector communication to the partitioning routine which did not exist in the original CuSP system.

Macrobatch Sampling The macrobatch sampler, the key to the system's performance, reduces sampling overhead by merging the communication that would occur over multiple minibatches into a single "macrobatch". This uses the fact that if excess memory is available on machines, it is possible to fetch the data for many minibatches at once. Fetched features must be static between minibatches (e.g., not learned as part of training) for macrobatch-fetched features to remain correct; this is not a problem for our use case where we train graphs with existing features. An epoch's M minibatches normally requires M communication relays in which the l -hop sampled subgraph and its features are

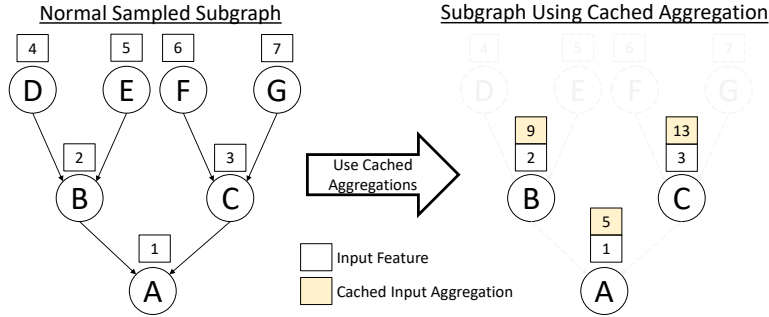


Figure 2: First compute layer’s subgraph with(out) cached aggregations. Subgraph edges and the last layer’s sampled nodes are not required in a subgraph with aggregated cached values.

requested and fetched. These relays block the communication process to wait for request responses. This slows the system. Therefore, instead of M relays for M minibatches, BatchGNN does one relay for B minibatches at once in a *macrobatch* of size B to reduce the number of communication relays by a factor of B . This reduces the number of communication barriers by a factor of B , and vertex properties shared by the different minibatches in the macrobatch are fetched only once.

The semantics of training are *not* changed by doing a macrobatch: all B minibatches are trained the same way they would be as if you fetched each one separately. The topology data fetched for a macrobatch of size B is the same as if you did all B batches one by one, but the features fetched are reduced based on the overlap of features fetched among the minibatches which depends on the vertices sampled in the macrobatch (Appendix A details a performance model for the expected benefits). BatchGNN also allows fetching features in batches of F (where $F \leq B$) when fetching features for all B batches at once is not possible due to memory constraints. This results in B/F feature fetching rounds instead of one. Our experiments assume $B = F$.

After sampling, BatchGNN exports homogeneous (i.e., untyped) sampled subgraphs into different graph representations. BatchGNN supports three representations: DGL [29], PyTorch Geometric (PyG) [7], and native BatchGNN. B minibatch subgraphs are exported to the user’s desired format, and training proceeds for those subgraphs before the next B batches are sampled.

Allocation-efficient Native Layers BatchGNN implements native GraphSAGE [11], GCN [20], 0- ϵ GIN [31], ReLU, and dropout layers that (1) reuse allocated buffer space for tensors and (2) track information required to do the backward phase to allow in-place operations. By reusing buffers and doing operations in-place, dynamic memory (de)allocation overhead is reduced. One limitation of buffer reuse is that the layers cannot be used with a different input before gradient computation because it would overwrite existing intermediate results needed for the backward phase. In practice, GNN layers are used only once before gradients are computed, so this is not a major problem.

Input Feature Aggregation Cache BatchGNN has optional construction of an *input feature aggregation cache* that pre-computes aggregations of static input features for use with BatchGNN GNN layers to reduce the computation and communication required during GNN training. Each machine constructs a cache which stores the aggregated feature of all neighbors for all vertices in the graph before any sampling occurs. BatchGNN-native GNN layers can fetch aggregated cached features of a vertex instead of doing aggregation over neighbors during the first GNN computational layer which uses these input features. Because the aggregations are cached, *there is no need to construct a subgraph with edges, do sampling, or do aggregation for the subgraph belonging to the first computational layer*. Figure 2 illustrates this: the constructed subgraph with cached aggregations only needs to fetch the aggregated feature for A , B , and C instead of the sampled nodes D through G , and no aggregation is required since cached features are already aggregated. This cache has limitations: (1) input features must be static, (2) fetching cached features for all nodes may fetch more data than fetching sampled node features, (3) there is initialization cost and memory overhead, and (4) since the cache does full aggregation instead of sampled aggregation and may estimate sampled subgraph degrees only known at runtime, training semantics are changed. Appendix B and Appendix C contains further discussion and a performance model for the cache.

Table 1: Inputs. arxiv/papers made undirected by adding the reverse edges.

	V	E	Feat.
arxiv	0.17M	2.3M	128
products	2.4M	123M	100
papers100M	111M	3.2B	128
LDBC1000	1.9B	13.5B	135

Table 2: Epoch time against P³ for 16 ranks, directed papers.

System	Time (s)
P³	3.1
BGNN	2.8

Table 3: Epoch time against DistDGLv2 for 64 ranks, undirected papers.

System	Time (s)
DistDGLv2	5.0
BGNN	4.5

4 Evaluation

4.1 Experimental Setup

The main experiments were run on up to 32 machines with a total of 72 Intel Xeon Platinum 8360Y (Ice Lake) CPU cores spread over 2 sockets with a total of 256 GB RAM. The machines are connected via Intel Omni-Path Architecture (OPA).

We compare BatchGNN against DistDGL (shortened to DGL henceforth) v1.0 [35]; both use PyTorch 1.12.1 [25]. For DistDGL, we do not alter its default multi-threading behavior nor specify additional sampler processes beyond the default 0. We run BatchGNN with (BGNNC) and without (BGNN) the aggregation cache and report them separately. The macrobatch size used by BatchGNN is large enough such that all minibatches of an epoch are fetched in 1 macrobatch *except* for papers on 2 ranks: 2 macrobatches are used in that setting to avoid the possibility of out-of-memory errors. Unless mentioned otherwise, the epoch time reported is for the third epoch of execution.

We use three GNN layers: GraphSAGE [11], GCN [20], and GIN [31]. For GCN and SAGE, we use 3 layers with a hidden feature size of 256. For GIN, we use 3 layers (without learnable epsilon to adjust the weight of the self-addition, i.e., $0-\epsilon$), and each GIN uses a 2-layer MLP with a hidden feature size of 256. The local minibatch size for each rank is 1024, and we sample with replacement with a sampling fan of 15, 10, 5 (where 15 is the number of samples from the initial minibatch vertices). Evaluation of the test vertices is done with a 20, 20, 20 sampling fan (sampling for test evaluation does not heavily affect accuracy [17]). An exception is made for GIN where we use the same fan as the training (15, 10, 5): we observed the GIN layer is sensitive to the parameters used during training, and changing them for testing results in poor accuracy. During test vertex evaluation, we *do not use the cache for GraphSAGE and GCN* (meaning the fixed-neighbor aggregations that testing sees differ from full-neighbor cached aggregations the model was trained with) but continue to use it for GIN (the reasoning is the same as the other GIN exception before) to keep the test comparison with DGL (which does not have a cache) the same. Reported speedups are an average over all configurations and GNN layers (i.e., including results in Appendix F.1) unless otherwise mentioned.

The specifications of the graphs that we experiment on are listed in Table 1 [3, 14]. For the OGBN graphs (arxiv, products, papers100M), the training/test splits are the defaults included with the OGB package [14]. arxiv and papers100M (henceforth shortened to “papers”) are directed graphs, so we make them undirected by adding the reverse edge for every edge. DGL’s symmetric version of arxiv and papers remove duplicates of edges with the same source and destination while BatchGNN keeps them (i.e., BatchGNN’s graph has more edges than DGL). products is already undirected. LDBC1000 [3] is a synthetic graph with generated features/labels used to show that BatchGNN can handle terabyte-scale graphs. We add random feature vectors of size 135 and make 80% of 1% of the vertices into training vertices. To partition the graphs, we use a random edge-cut partition for both BatchGNN and DGL. DGL supports METIS partitioning, but for a fair comparison with BatchGNN, we use random DGL for the main experiments. As a special case, we show the runtime of DGL with METIS partitions (denoted DGL-M) for papers on 32 hosts to discuss the differences with METIS.

The full experimental setup can be found Appendix E. The Appendix also contains more experimental results and detailed analysis to supplement the results presented in this section.

Table 4: Average runtime (seconds) and breakdown of distributed GNN training for 1 epoch. Prep time includes time to prepare a subgraph: topology sampling, feature fetching, and export.

Graph	Ranks	System	SAGE						
			Subgraph Prep			Compute		Epoch Total	
			Topo	Feat	Export	Total	Fwd		Bwd
arxiv	4	DGL	0.76	0.33	-	1.10	0.25	0.48	1.87
		BGNN	0.11	0.10	0.04	0.26	0.32	0.58	1.19
		BGNNC	0.11	0.07	0.03	0.22	0.34	0.44	1.03
products	8	DGL	3.21	4.48	-	7.70	0.84	3.30	11.88
		BGNN	0.45	0.73	0.31	1.52	0.71	0.86	3.12
		BGNNC	0.65	0.44	0.14	1.25	0.61	0.86	2.74
papers	32	DGL	5.64	21.49	-	27.13	1.08	13.66	41.96
		DGL-M	4.51	12.55	-	17.06	0.94	16.93	35.02
		BGNN	0.55	2.76	0.45	3.79	0.99	1.81	6.64
		BGNNC	1.41	1.06	0.15	2.65	0.86	2.17	5.73

Table 5: Number of feature vectors fetched among all machines for various OGBN graphs.

Graph	Ranks	System	Fetched	V
arxiv	4	DGL	3.9M	0.2M
		BGNN	0.5M	
		BGNNC	0.8M	
products	8	DGL	68.0M	2.4M
		BGNN	12.2M	
		BGNNC	15.2M	
papers	32	DGL	463.6M	111.1M
		DGL-M	249.2M	
		BGNN	183.6M	
		BGNNC	127.4M	

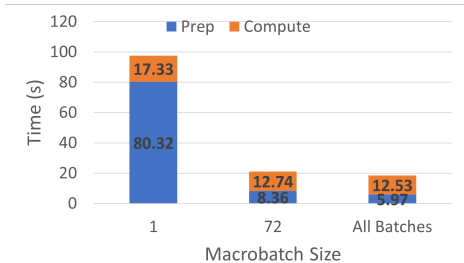


Figure 3: SAGE epoch time on LDBC1000 on 48 ranks with varying macrobatch sizes (average among ranks of 3 runs).

4.2 Epoch Time Overview

BatchGNN achieves better performance than DGL on CPUs and GPU systems DistDGLv2 [36] and P³ [9]. Macrobatching significantly reduces subgraph preparation time (subgraph sampling, feature fetching, and subgraph export) and mitigates load imbalance effects on runtime.

Comparison with DistDGL Table 4 shows the epoch time and the breakdown of training for the OGBN graphs on DGL and BatchGNN without (BGNN) and with (BGNNC) the aggregation cache for the SAGE layer for 4 ranks for arxiv, 8 ranks for products, and 32 ranks for papers (Appendix F.1 contains our full results for all configurations and layers). BGNN outperforms DGL significantly: it has a geometric mean speedup of 3× over DGL over all configurations and GNN layers types.

The main reason for the speedup is macrobatch sampling. Table 5 shows the number of features fetched in an epoch, and DGL fetches 7.8×, 5.6×, and 2.5× more features than BGNN does for arxiv, products, and papers, respectively, for the settings shown in Table 4. BGNN combines the fetches of multiple minibatches into a macrobatch to reduce redundant fetches. As a result, BGNN’s fetching time is much faster than DGL’s: on average, BGNN’s prep time is 6× faster than DGL’s.

DGL-M is faster than DGL because the METIS partitioning results in smaller sampled subgraphs and fewer remote feature fetches. METIS places vertices to reduce cross-partition edges which results in the seeds of a partition being closer together in topology. Since more neighbors are shared due to locality, the number of sampled vertices in a subgraph decreases and results in smaller subgraphs. This fact combined with fewer cross-partition edges (i.e., subgraph consists of more local vertices) results in fewer remote fetches (see Table 5) and lower subgraph prep time. However, even with METIS, DGL-M is still slower than and fetches more features than BGNN.

The memory optimizations that BatchGNN implements in its native GNN layers can result in slight improvement in runtime for a larger graph like papers. For arxiv, however, note that BGNN’s native layer is actually slower than DGL, so the optimizations are not necessarily always effective. The native layer can still be advantageous, however, because it allows BatchGNN to avoid conversion overhead to a DGL/PyG subgraph and integrates with the aggregation cache (BGNNC).

Comparison with GPU Systems Table 2 and Table 3 compare BatchGNN against runtimes reported in the P³ [9] and DistDGLv2 [36] papers, respectively. BatchGNN is run with the training setting described in those papers to the best of our knowledge (i.e., set the parameters we are aware of to same as theirs). For the P³ comparison, we ran a 2-layer SAGE model with fan (25, 10), hidden feature size 32 on 16 ranks on *directed* papers with in-edge sampling to compare against P³’s run on 16 NVIDIA P100 GPUs. For the DistDGLv2 comparison, we ran a 3-layer SAGE model with fan (15, 10, 5), hidden feature size 256 on 64 ranks on undirected papers to compare against DistDGLv2’s run on 64 NVIDIA T4 GPUs. For both cases, we sample with replacement and use a minibatch size of 1000. As shown in the tables, BatchGNN outperforms the reported runtimes for those GPU systems.

Effects of Load Imbalance Observe in Table 4 that DGL’s backward phase time for is significantly higher than BGNN’s: the reason for this is heavy load imbalance in execution. Imbalance in sampling runtime and forward computation can increase backward time for all ranks if there is a single rank slower than other ranks as backward computation involves a barrier to synchronize gradients. We observed in our experiments that DGL has very heavy imbalance among ranks which results in high barrier wait time. This results in a slower epoch. In addition, the reason that DGL-M does not result in a larger performance improvement over DGL can be explained with imbalance as well. We observed METIS partitions result in more relative imbalance than random partitions, so the backward time in Table 4 for DGL-M is higher than that of normal DGL. BatchGNN does not have this problem: its ranks are relatively balanced. Any sampling imbalance only occurs when fetching macrobatches rather than for every minibatch in the macrobatch. Macrobatching *mitigates* the effect of imbalance because sampling does not occur past the first minibatch of a macrobatch. When minibatches are sampled one at a time like in DGL, sampling imbalance reoccurs for every minibatch, *amplifying* the imbalance. Therefore, macrobatching can improve runtime by mitigating load imbalance overheads. Experimental results quantifying this imbalance and further discussion can be found in Appendix F.2.

LDBC1000 and Effects of Macrobath Size We run BatchGNN on LDBC1000 [3] with added synthetic features and labels on 48 hosts to (1) show that BatchGNN scales out by running it on a terabyte-scale graph and (2) to experiment with variations on macrobatch size and highlight the effects on execution time. In particular, we use SAGE with BGNN with the same hyperparameters our main set of experiments except with variations on macrobatch size. We select macrobatch size 1, 72, and all minibatches (e.g. ≥ 304). Figure 3 shows the results of this experiment.

Macrobath size 1 is the slowest and has significantly higher subgraph preparation (sampling, feature fetching, and export) time than the other two settings. Because sampling occurs for every minibatch, redundant features may be fetched across minibatches since they are not fetched for multiple minibatches at once. To illustrate this, we collected the number of remote features vectors fetched in an epoch for these settings: macrobatch size 1 fetches 596M, macrobatch size 72 fetches 464M, and all batches fetches 363M. Macrobatching reduces the total number of features that need to be fetched. Additionally, imbalance in subgraph preparation is amplified at lower macrobatch sizes as discussed previously. This may result in slower compute time due to imbalance and the barrier that exists for gradient synchronization. Most importantly, BatchGNN cannot fully leverage parallelism during subgraph preparation in the single minibatch setting because parallelism is interbatch: if there is only a single minibatch to prepare, there will be single threaded execution during subgraph preparation (Appendix D.3 discusses this implementation detail). At macrobatch size 72, there are 72 minibatches for the 72 threads on the machine to work on at the same time. Combined with less redundant feature fetching, macrobatch size 72 has significantly improved runtime over the size 1 setting. Finally, the all-batch setting reduces the communication overhead further and results in the fastest run in this experiment.

Runtime with Aggregation Cache BGNNC is BatchGNN with the aggregation cache enabled, and as shown Table 4, it typically reduces the runtime of the epoch by reducing the time taken by subgraph preparation. On average, an epoch is $1.2\times$ faster in BGNNC than BGNN. Instead of sampling and

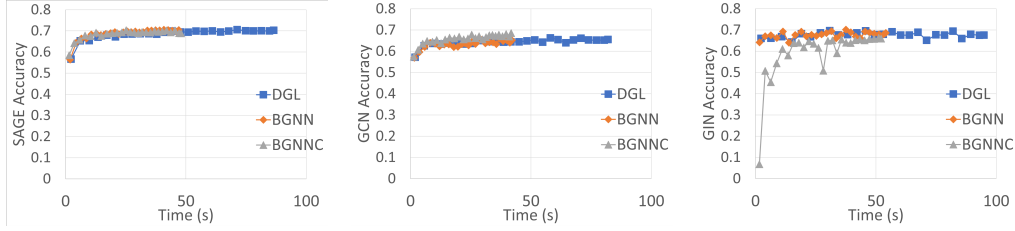


Figure 4: Time (sec) to accuracy, arxiv, 4 ranks, for SAGE, GCN, and GIN, respectively.

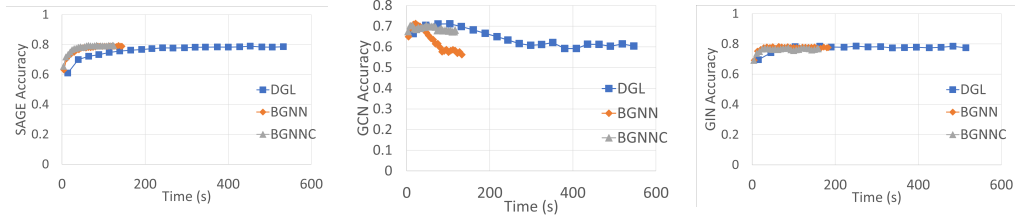


Figure 5: Time (sec) to accuracy, products, 8 ranks, for SAGE, GCN, and GIN, respectively.

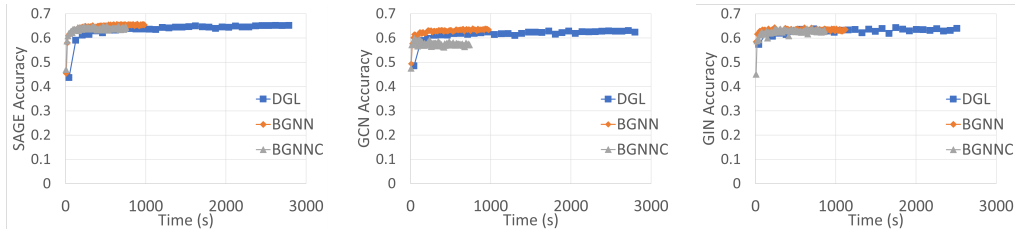


Figure 6: Time (sec) to accuracy, papers, 32 ranks, for SAGE, GCN, and GIN, respectively.

fetching for the last sampling layer, the system fetches remote aggregated features. This remote fetch time is included in the “Topo” column of the preparation time, and the change in the number of input features fetched is reflected in the reduction of the time in the “Feat” column for BGNNC.

The cache is not guaranteed to significantly reduce epoch time. Table 5 explains this: for arxiv and products, the cache variant fetches more features than the no-cache variant. This is possible if sampling does not add many new vertices since the aggregation cache must fetch aggregated features for all vertices instead of fetching only non-cached features from newly sampled nodes (see Appendix C for the performance model). Fetching more features means (1) more communication overhead during the subgraph preparation and (2) potentially more feature reads during the forward phase when fetching the aggregated cached values than reads that would have occurred in the non-cached case. Both can add enough overhead such that it outweighs the benefits of skipping the aggregation step and reducing export time.

4.3 Time to Accuracy

Figure 4, Figure 5, and Figure 6 show accuracy plots for each graph and model (we drop some later points for DGL because it takes longer to run the same number of epochs). We did not optimize hyperparameters for accuracy: these results are to compare convergence behavior of the systems. BGNN achieves similar accuracy to DGL at a faster rate. Minor convergence differences are expected due to the randomness of sampling and training as well as possible low-level implementation differences in the GNN layers (high-level semantics are the same).

Since BGNNC uses full-neighbor aggregation and estimated normalization for GCN, the convergence of BGNNC differs from that of BGNN. The effect on accuracy depends on setting it is run under: there are instances of it improving accuracy, maintaining accuracy, and decreasing accuracy. For example, the cache increases accuracy for GCN on arxiv, but it decreases it for GIN on all graphs.

Therefore, the aggregation cache’s effectiveness should be evaluated on a case-by-case basis: in exchange for a change in semantics and accuracy change, the runtime of an epoch can be decreased.

5 Conclusion

We presented BatchGNN, an scalable end-to-end distributed GNN training system for CPUs that achieves state-of-the-art performance. Macrobatching does sampling and feature fetching of many minibatches in a single communication relay to reduce the number of communication relays and redundant feature fetches. In addition to macrobatching, it implements an aggregation cache to reduce sampling costs for the first computational layer, integrated on-demand graph partitioning, and memory-aware native GNN layers which all serve to reduce end-to-end training time. It is $3\times$ faster than DistDGL, outperforms distributed GPU GNN systems P³ and DistDGLv2 using only CPUs, and permits terabyte-size graph training via scale-out. The ideas presented in BatchGNN can be applied to existing distributed CPU and GPU GNN systems that use sampling to accelerate training.

References

- [1] *A Graph Neural Network Approach for Product Relationship Prediction* (08 2021), vol. Volume 3A: 47th Design Automation Conference (DAC) of *International Design Engineering Technical Conferences and Computers and Information in Engineering Conference*. V03AT03A036.
- [2] ALIBABA. Euler, Distributed Graph Deep Learning Framework.
- [3] ANGLES, R., ANTAL, J. B., AVERBUCH, A., BONCZ, P. A., ERLING, O., GUBICHEV, A., HAPRIAN, V., KAUFMANN, M., LARRIBA-PEY, J.-L., MARTINEZ-BAZAN, N., MARTON, J., PARADIES, M., PHAM, M.-D., PRAT-PEREZ, A., SPASIC, M., STEER, B. A., SZARNYAS, G., AND WAUDBY, J. The LDBC Social Network Benchmark.
- [4] BONGINI, P., BIANCHINI, M., AND SCARSELLI, F. Molecular generative Graph Neural Networks for Drug Discovery. *Neurocomputing* 450 (2021), 242–252.
- [5] CHEN, J., MA, T., AND XIAO, C. FastGCN: Fast Learning with Graph Convolutional Networks via Importance Sampling. In *International Conference on Learning Representations* (2018).
- [6] DOU, Y., LIU, Z., SUN, L., DENG, Y., PENG, H., AND YU, P. S. Enhancing Graph Neural Network-Based Fraud Detectors against Camouflaged Fraudsters. In *Proceedings of the 29th ACM International Conference on Information and Knowledge Management (New York, NY, USA, 2020)*, CIKM ’20, Association for Computing Machinery, p. 315–324.
- [7] FEY, M., AND LENSSEN, J. E. Fast Graph Representation Learning with PyTorch Geometric. In *ICLR Workshop on Representation Learning on Graphs and Manifolds* (2019).
- [8] FEY, M., LENSSEN, J. E., WEICHERT, F., AND LESKOVEC, J. GNNAutoScale: Scalable and Expressive Graph Neural Networks via Historical Embeddings. In *Proceedings of the 38th International Conference on Machine Learning (18–24 Jul 2021)*, M. Meila and T. Zhang, Eds., vol. 139 of *Proceedings of Machine Learning Research*, PMLR, pp. 3294–3304.
- [9] GANDHI, S., AND IYER, A. P. P3: Distributed Deep Graph Learning at Scale. In *15th USENIX Symposium on Operating Systems Design and Implementation (OSDI 21)* (July 2021), USENIX Association, pp. 551–568.
- [10] GASTEIGER, J., QIAN, C., AND GÜNNEMANN, S. Influence-Based Mini-Batching for Graph Neural Networks. In *The First Learning on Graphs Conference* (2022).
- [11] HAMILTON, W. L., YING, Z., AND LESKOVEC, J. Inductive Representation Learning on Large Graphs. In *NIPS* (2017), pp. 1024–1034.
- [12] HOANG, L., CHEN, X., LEE, H., DATHATHRI, R., GILL, G., AND PINGALI, K. Efficient Distribution for Deep Learning on Graphs. In *First MLSys Workshop on Graph Neural Networks and Systems (GNNSys21)* (2021).

- [13] HOANG, L., DATHATHRI, R., GILL, G., AND PINGALI, K. CuSP: A Customizable Streaming Edge Partitioner for Distributed Graph Analytics. In *Proceedings of the 33rd IEEE International Parallel and Distributed Processing Symposium* (2019), IPDPS 2019, pp. 439–450.
- [14] HU, W., FEY, M., ZITNIK, M., DONG, Y., REN, H., LIU, B., CATASTA, M., AND LESKOVEC, J. Open Graph Benchmark: Datasets for Machine Learning on Graphs. In *Advances in Neural Information Processing Systems* (2020), H. Larochelle, M. Ranzato, R. Hadsell, M. F. Balcan, and H. Lin, Eds., vol. 33, Curran Associates, Inc., pp. 22118–22133.
- [15] INTEL. Intel oneAPI Math Kernel Library.
- [16] JIA, Z., LIN, S., GAO, M., ZAHARIA, M., AND AIKEN, A. Improving the Accuracy, Scalability, and Performance of Graph Neural Networks with Roc. In *Proceedings of Machine Learning and Systems* (2020), I. Dhillon, D. Papailiopoulos, and V. Sze, Eds., vol. 2, pp. 187–198.
- [17] KALER, T., STATHAS, N., OUYANG, A., ILIOPOULOS, A.-S., SCHARDL, T., LEISERSON, C. E., AND CHEN, J. Accelerating Training and Inference of Graph Neural Networks with Fast Sampling and Pipelining. In *Proceedings of Machine Learning and Systems* (2022), D. Marculescu, Y. Chi, and C. Wu, Eds., vol. 4, pp. 172–189.
- [18] KARYPIS, G., AND KUMAR, V. A Fast and High Quality Multilevel Scheme for Partitioning Irregular Graphs. *SIAM J. Sci. Comput.* 20, 1 (Dec. 1998), 359–392.
- [19] KESKAR, N. S., MUDIGERE, D., NOCEDAL, J., SMELYANSKIY, M., AND TANG, P. T. P. On Large-Batch Training for Deep Learning: Generalization Gap and Sharp Minima, 2016.
- [20] KIPF, T. N., AND WELLING, M. Semi-Supervised Classification with Graph Convolutional Networks. In *ICLR* (2017).
- [21] MA, L., YANG, Z., MIAO, Y., XUE, J., WU, M., ZHOU, L., AND DAI, Y. NeuGraph: Parallel Deep Neural Network Computation on Large Graphs. In *2019 USENIX Annual Technical Conference (USENIX ATC 19)* (Renton, WA, July 2019), USENIX Association, pp. 443–458.
- [22] MD, V., MISRA, S., MA, G., MOHANTY, R., GEORGANAS, E., HEINECKE, A., KALAMKAR, D., AHMED, N. K., AND AVANCHA, S. DistGNN: Scalable Distributed Training for Large-Scale Graph Neural Networks. In *Proceedings of the International Conference for High Performance Computing, Networking, Storage and Analysis* (New York, NY, USA, 2021), SC ’21, Association for Computing Machinery.
- [23] NGUYEN, D., LENHARTH, A., AND PINGALI, K. A Lightweight Infrastructure for Graph Analytics. In *Proceedings of the Twenty-Fourth ACM Symposium on Operating Systems Principles* (New York, NY, USA, 2013), SOSP ’13, ACM, pp. 456–471.
- [24] PARK, Y., MIN, S., AND LEE, J. W. Ginex: SSD-enabled Billion-scale Graph Neural Network Training on a Single Machine via Provably Optimal In-memory Caching. In *Proceedings of the VLDB Endowment* (2022), vol. 15.
- [25] PASZKE, A., GROSS, S., MASSA, F., LERER, A., BRADBURY, J., CHANAN, G., KILLEEN, T., LIN, Z., GIMELSHEIN, N., ANTIGA, L., DESMAISON, A., KOPF, A., YANG, E., DEVITO, Z., RAISON, M., TEJANI, A., CHILAMKURTHY, S., STEINER, B., FANG, L., BAI, J., AND CHINTALA, S. PyTorch: An Imperative Style, High-Performance Deep Learning Library. In *Advances in Neural Information Processing Systems 32*, H. Wallach, H. Larochelle, A. Beygelzimer, F. d’Alché-Buc, E. Fox, and R. Garnett, Eds. Curran Associates, Inc., 2019, pp. 8026–8037.
- [26] TRIPATHY, A., YELICK, K., AND BULUÇ, A. Reducing Communication in Graph Neural Network Training. In *Proceedings of the International Conference for High Performance Computing, Networking, Storage and Analysis* (2020), SC ’20, IEEE Press.
- [27] VELIČKOVIĆ, P., CUCURULL, G., CASANOVA, A., ROMERO, A., LIÒ, P., AND BENGIO, Y. Graph Attention Networks. In *ICLR* (2018).

- [28] WAN, C., LI, Y., LI, A., KIM, N. S., AND LIN, Y. BNS-GCN: Efficient Full-Graph Training of Graph Convolutional Networks with Partition-Parallelism and Random Boundary Node Sampling. In *Proceedings of Machine Learning and Systems (2022)*, D. Marculescu, Y. Chi, and C. Wu, Eds., vol. 4, pp. 673–693.
- [29] WANG, M., YU, L., ZHENG, D., GAN, Q., GAI, Y., YE, Z., LI, M., ZHOU, J., HUANG, Q., MA, C., HUANG, Z., GUO, Q., ZHANG, H., LIN, H., ZHAO, J., LI, J., SMOLA, A. J., AND ZHANG, Z. Deep Graph Library: Towards Efficient and Scalable Deep Learning on Graphs. In *International Conference on Learning Representations (2019)*, ICLR '19.
- [30] XU, J., BAI, Z., FAN, W., LAI, L., LI, X., LI, Z., QIAN, Z., WANG, L., WANG, Y., YU, W., AND ZHOU, J. GraphScope: A One-Stop Large Graph Processing System. *Proc. VLDB Endow.* 14, 12 (oct 2021), 2703–2706.
- [31] XU, K., HU, W., LESKOVEC, J., AND JEGELKA, S. How Powerful are Graph Neural Networks? In *International Conference on Learning Representations (2019)*, ICLR '19.
- [32] YANG, H. AliGraph: A Comprehensive Graph Neural Network Platform. In *Proceedings of the 25th ACM SIGKDD International Conference on Knowledge Discovery & Data Mining (New York, NY, USA, 2019)*, KDD '19, Association for Computing Machinery, pp. 3165–3166.
- [33] ZENG, H., ZHOU, H., SRIVASTAVA, A., KANNAN, R., AND PRASANNA, V. Accurate, Efficient and Scalable Graph Embedding. In *2019 IEEE International Parallel and Distributed Processing Symposium (IPDPS) (May 2019)*, pp. 462–471.
- [34] ZHENG, C., CHEN, H., CHENG, Y., SONG, Z., WU, Y., LI, C., CHENG, J., YANG, H., AND ZHANG, S. ByteGNN: Efficient Graph Neural Network Training at Large Scale. *Proc. VLDB Endow.* 15, 6 (feb 2022), 1228–1242.
- [35] ZHENG, D., MA, C., WANG, M., ZHOU, J., SU, Q., SONG, X., GAN, Q., ZHANG, Z., AND KARYPIS, G. DistDGL: Distributed Graph Neural Network Training for Billion-Scale Graphs, 2021.
- [36] ZHENG, D., SONG, X., YANG, C., LASALLE, D., AND KARYPIS, G. Distributed Hybrid CPU and GPU Training for Graph Neural Networks on Billion-Scale Heterogeneous Graphs. In *Proceedings of the 28th ACM SIGKDD Conference on Knowledge Discovery and Data Mining (New York, NY, USA, 2022)*, KDD '22, Association for Computing Machinery, p. 4582–4591.
- [37] ZOU, D., HU, Z., WANG, Y., JIANG, S., SUN, Y., AND GU, Q. Layer-Dependent Importance Sampling for Training Deep and Large Graph Convolutional Networks. In *Advances in Neural Information Processing Systems (2019)*, H. Wallach, H. Larochelle, A. Beygelzimer, F. d'Alché-Buc, E. Fox, and R. Garnett, Eds., vol. 32, Curran Associates, Inc.

What follows is the Appendix for the paper BatchGNN: Efficient CPU-Based Distributed GNN Training on Very Large Graphs.

A Macrobatching Performance Model

This section analyzes the potential performance gain of macrobatching.

Let C be the incidental data cost (e.g., confirmation messages, metadata, etc.) of doing a communication relay for subgraph sampling. Let T_i be the size of the topology data for minibatch i . Let f_i be the set of vertices to fetch for minibatch i . Assume for the sake of worst-case analysis that all node features are fetched from another machine. Let S be the size of the initial feature vector. For a total of M minibatches, the communication cost is the following:

$$\sum_{i=0}^{M-1} T_i + MC + \sum_{i=0}^{M-1} S * count(f_i) \tag{2}$$

Let B be the macrobatch size. Let A_k be the union of all vertices to fetch for minibatches $k * B$ through $(k + 1) * B - 1$ (i.e., union of B minibatches).

$$\sum_{i=0}^{M-1} T_i + \frac{MC}{B} + \sum_{k=0}^{\frac{M}{B}-1} S * count(A_k) \tag{3}$$

The incidental data cost is reduced by a factor of B , and the feature data is reduced by the amount of overlap in features of the B minibatches in the macrobatch. Therefore, if there is a high overlap, macrobatching significantly reduces sampling overhead. The reduction in the number of relays (i.e., barriers among all machines) and incidental data costs provide benefit as well.

B Further Aggregation Cache Discussion

The cache is constructed once and can be reused indefinitely if the input features to a GNN model never change and if the graph does not add new nodes and/or edges. Otherwise, cache elements may become invalid and would need to be updated. BatchGNN currently only trains static graphs without learnable inputs, so these problems are avoided. The aggregation cache can only be used with BatchGNN native layers since the layer must be aware that the cache exists to use it. Other GNN layers from other systems like DGL would need to be modified to allow the use of the cache.

In addition, training semantics change with the aggregation cache. Instead of aggregating over a sampled set of neighbors during compute, the cached aggregated value which results from aggregating over *all* neighbors is used instead. As a result, training changes since the aggregated value for the first GNN layer will always be the same instead of being dependent on the sampled neighbors (i.e., no variation during training). The result is a semantically different hybrid computational scheme where the first computational layer uses full neighbor aggregation (theoretically, more neighborhood information is used) while the following layers use sampled aggregation. Also, some types of aggregation normalization like symmetric normalization used by GCN require knowledge of the subgraph at *runtime* which is not known at cache construction time. Specifically, the degrees of nodes being aggregated from are not known until the graph is sampled, and this metric is required for correct symmetric normalization. In our implementation, we estimate this value at cache construction time using global degrees. This will change training semantics.

C Aggregation Cache Performance Model

We analyze the possible performance gain with the aggregation cache.

Let V be the set of vertices that need to be sampled from to create the subgraph for the first computational layer, S be the size of the initial feature vector, $\mathcal{N}(V)$ be the set of vertices not in V that are selected as a result of neighbor sampling for the layer, T_v be the size of the vertex data for

vertices in V , T_n the size of the vertex data for vertices in $\mathcal{N}(V)$, and T_e be the size of the edge data for the subgraph.

The data cost for constructing the subgraph includes the input features for all vertices in the graph and the topology data:

$$VS + \text{count}(\mathcal{N}(V)) * S + T_v + T_n + T_e \tag{4}$$

When using the cache, the data cost is instead the following.

$$VS + VS + T_v \tag{5}$$

The initial input features of V are still be fetched because some layers require it, but the cost of fetching sampled vertices, their features, and sampled edges is eliminated since they do not need to be sampled nor created. Instead, all cached aggregated features are fetched (the VS term). Therefore, the aggregation cache reduces communicated data volume if V is smaller than $\mathcal{N}(V)$. There are scenarios where this is not the case: for example, if the number of newly sampled nodes is low because all nodes have already been sampled by the last layer, then using the cache requires communication of significantly more data. Regardless of the data savings, the use of the cache eliminates the sampling phase as well as the aggregation step in the first GNN layer. This can have beneficial performance implications.

D System Implementation Details

This section goes into detail of selected aspects of the implementation of BatchGNN’s macrobatch sampler to allow for better understanding of the system’s performance.

D.1 Parallel Topology Sampling

Efficient neighborhood sampling is accomplished by preallocating as many communication buffers and edge buffers as possible to allow multiple threads to write their individual sampling results without the need for dynamic memory allocation. The high-level steps involved in BatchGNN’s neighborhood sampling for a layer are (1) determining vertices to sample (known as *seed vertices*) and the machines that own the edges for them (2) making requests to those machines to sample those vertices, (3) fulfilling the sampling requests and sending the sampled neighbors and edges back to the requester, and (4) processing the fulfilled requests. This subsection will highlight selected areas of this pipeline.

D.1.1 Generating Request Messages

Given a set of unique vertices for each of the B minibatches in a macrobatch, BatchGNN determines which machine owns the edges for each vertex and constructs a request message for each machine in parallel via an inspector-executor pattern. A Galois [23] parallel loop construct is used to loop over each minibatch’s seed vertices in parallel. Each thread notes the owner machine of the vertex it inspects, and a thread-local count for the number of vertices to request from that machine is incremented. Once this first loop concludes, memory for a message buffer for each machine is allocated as the system knows exactly how many requests to make to each machine by summing the thread-local counts. The minibatches are then iterated over again in parallel using the same thread assignment as the inspector phase, and by using the thread-local counts, each thread can serialize vertex IDs into disjoint locations of the message buffer for a machine because the exact number each thread writes for each machine is known from inspection. The minibatch ID and the seed index for the vertex being serialized for index i of the buffer is maintained while doing this serialization, to associate each vertex with the location to store its results later.

If the input feature aggregation cache is enabled for use with native BatchGNN GNN layers, sampling does not occur for the last sampling layer (i.e., the first computational layer). Instead, the system fetches the required aggregated features for that layer’s seed vertices, eliminating the need for sampling and compute during computation (see Section 3 of the main paper).

D.1.2 Sampling Request Fulfillment

Machines receive sampling requests that can be handled efficiently by preallocating all necessary memory for the response in parallel. Upon receipt of a request message, the memory for the response message is allocated based on the number of vertices requested. The memory is a known amount because (1) the sampling is fixed-neighbor, so the (maximum) number of neighbors is known or (2) all neighbors are being requested, and the degree of the vertex is known. Each requested vertex ID is then added to a thread-safe Galois sampling worklist which consists of requested vertices from all machines along with a pointer into the response message memory designating where sampled vertices and edges are to be written. This ensures that there is no redundant copying since results are written directly into the buffer to be sent and that the thread working on that vertex will not interfere with the writes from other threads. Once the response buffers are allocated and the worklist is constructed, parallel topology sampling occurs over the worklist. Each thread takes a worklist item, does sampling for the item's vertex, and writes the results into the item's saved pointer. The result is parallel sampling for all minibatches in the macrobatch among all machines in the network. Graph access locality can also be better leveraged since sampling occurs in one macrobatch rather than across B individual minibatches. Once finished, each machine sends back the sampled vertices and edges in the same order that the requester requested the vertices.

D.1.3 Processing Received Sampled Vertices and Edges

Because the minibatch and seed indices were saved when generating the request message (Appendix D.1.1), it is simple to deserialize the sampled results from other machines into the correct locations upon receipt since are sent back in the same order. A parallel loop is used to iterate over each request response, and the index of the vertex being processed in the buffer links it to the minibatch and seed index to write the sampled results into based on the agreed-upon order of messages. The storage for result deserialization will have been preallocated if the number of sampled neighbors is fixed. When sampling does not involve a fixed neighbor such as in full-neighbor sampling where all neighbors of a vertex are fetched, this storage is allocated when the degrees of the vertices being sampled are sent to the requester (the degrees are not sent if they are not required).

D.2 Property Fetching and Subgraph Export

Properties (e.g., labels, features) are fetched in batches on demand whenever an exported subgraph for a minibatch is requested. When a single minibatch subgraph is requested, a batch is created at once. This subsection describes how both occur.

D.2.1 Property Fetching

Given a macrobatch with B minibatches, BatchGNN fetches properties for F of those minibatches in a batch to avoid fetching redundant properties among the subgraphs of the minibatches and to reduce the number of communication barriers required. First, a set of all unique vertices (and edges, if required) is compiled in parallel by threads checking all minibatches and adding their vertices to a concurrent set data structure. This set is used to do distributed feature fetching: an all-to-all fetching operation pulls all remote properties as well as local properties for the vertices in the set into a single array for each fetched property. A mapping from vertex ID to its corresponding index in these arrays is created as well. At this point, the properties for all entities in the B minibatched subgraphs exist on each machine.

D.2.2 Subgraph Export

BatchGNN exports F subgraphs (the number of minibatches that features are fetched for) in parallel to a structure in which it can be used with the BatchGNN native layer implementations or to a structure that is more friendly for further transformation into a DGL or PyTorch Geometric (PyG) subgraph (we will refer to it as a Python subgraph) for use with those systems. For a native layer subgraph, the sampled edges are exported into a compressed sparse row (CSR) format for efficient parallel iteration over individual vertices' edges, and the transpose (a compressed sparse column, CSC) graph is created as well to do reverse aggregation in the backward phase. For the Python subgraph, the edges are placed into an Arrow tensor objects because Arrow tensor objects can be zero-copied to PyTorch tensors which DGL/PyG use for edges. The Python subgraphs undergo further processing as

necessary to convert them to the DGL/PyG graph format upon use. All subgraphs also require that the initial vertex features be placed into a contiguous array as well. The features for the subgraph’s vertices are copied from the F -minibatch property array using the mapping from ID to index to select the correct features. The features are stored in an Arrow array for zero-copy to PyTorch.

D.3 Discussion: Inter- vs Intra-batch Parallelism

BatchGNN’s sampler uses interbatch parallelism (threads work on individual minibatches) rather than intrabatch parallelism (threads work on the same minibatch). If there are a low number of minibatches in a macrobatch, all threads may not be fully utilized. BatchGNN is not expected to perform well in this scenario.

Minibatches are typically small, so there is not much benefit assigning many threads to work on a single minibatch. In addition, intrabatch parallelism may require the use of atomics, locks, or additional thread-safe data structures to allow multiple threads to work on a task at once in a minibatch. For example, in construction of the CSR for native layer export, the counting of the number of edges for each vertex would need to be an atomic variable which would likely outweigh the benefits of intrabatch parallelism. By allowing threads to work on disjoint subgraphs of a macrobatch, more work can be accomplished faster with better thread utilization, and additional overhead from thread-safe constructs is avoided.

E Full Experimental Setup

The following is the unabridged experimental setup with none of the details omitted for purposes of space limits. Portions of this text can also be found in the main paper.

The main experiments were run on up to 32 machines with a total of 72 Intel Xeon Platinum 8360Y (Ice Lake) CPU cores spread over 2 sockets with a total of 256 GB RAM. The machines are connected via Intel Omni-Path Architecture (OPA).

We compare BatchGNN against DistDGL (shorted to DGL henceforth) v1.0 [35]. Both use PyTorch 1.12.1 [25]. Every machine runs a single trainer process (i.e., 1 rank per machine) for both systems. In DistDGL’s case, we do not alter its default multi-threading behavior, and we do not specify additional sampler processes beyond the default setting of 0. We run BatchGNN with (BGNNC) and without (BGNN) the aggregation cache and report them separately. The macrobatch size used by BatchGNN is large enough such that all minibatches of an epoch are fetched in 1 macrobatch *except* for papers on 2 ranks: 2 macrobatches are used in that setting to avoid the possibility of out-of-memory errors. We do not show results for BatchGNN’s export into DGL/PyG subgraphs with computation with their respective layers because the key contributions of our system are the sampler and the native layers. Reported numbers are not the first epoch of execution but the third because the first epoch can be slower than the rest. For BatchGNN in particular, the first epoch is when the initial reallocation of memory occurs for the native layer. On average, the third epoch for BatchGNN is $1.27\times$ faster than the first epoch for the main experiments of this paper, and at worst, the third epoch is $1.87\times$ faster than the first. Unless otherwise mentioned, times are average across all ranks of an epoch for each category (prep, forward, etc.).

We use three GNN layers: GraphSAGE [11], GCN [20], and GIN [31]. For GCN and SAGE, we use 3 layers (with ReLU/Dropout for the first two layers) with a hidden feature size of 256. For GIN, we use 3 layers (without learnable epsilon to adjust the weight of the self-addition, i.e., $0-\epsilon$), and each GIN uses a 2-layer MLP with a hidden feature size of 256 with batch normalization and ReLU after the first layer of the MLP. Each GIN layer does another batch normalization followed by a ReLU at the end. We do not optimize the hyperparameters for accuracy because evaluating the accuracy of different models is not the purpose of this work. However, we do report accuracy to make sure that the native layer implementations in BatchGNN result in similar accuracy to DistDGL. The local minibatch size for each rank is 1024, and we sample with replacement with a sampling fan of 15, 10, 5 (where 15 is the number of samples from the initial vertices of the minibatch). Evaluation of the test vertices is done with a 20, 20, 20 sampling fan (sampling for test evaluation does not heavily affect accuracy [17]). An exception is made for GIN where we use the same fan as the training (15, 10, 5): we observed the GIN layer is sensitive to the parameters used during training, and changing them for testing results in poor accuracy. Using the aggregation cache means that the last sampling

layer’s fan (5) is ignored in favor of the use of the full-neighbor cached aggregated value during training. During test vertex evaluation, we *do not use the cache for GraphSAGE and GCN* (meaning the fixed-neighbor aggregations that testing sees differ from full-neighbor cached aggregations the model was trained with) but continue to use it for GIN (the reasoning is the same as the other GIN exception before) to keep the test comparison with DGL (which does not have a cache) the same when it does not heavily affect accuracy like GIN.

The specifications of the graphs that we experiment on are listed in Table 1 [3, 14] of the main paper. For the OGBN graphs (arxiv, products, papers100M), the training/test splits are the defaults included with the OGB package [14]. arxiv and papers100M (henceforth shortened to “papers”) are directed graphs, so we make them undirected by adding the reverse edge for every edge. DGL’s symmetric version of arxiv and papers remove duplicates of edges with the same source and destination while BatchGNN keeps them (i.e., BatchGNN’s graph has more edges than DGL). products is already undirected. LDBC1000 [3] is a synthetic graph with generated features/labels used to show that BatchGNN can handle terabyte-scale graphs. We add random feature vectors of size 135 and make 80% of 1% of the vertices into training vertices. To partition the graphs, we use a random edge-cut partition for both BatchGNN and DGL. DGL supports METIS partitioning, but for a fair comparison with BatchGNN, we use random DGL for the main experiments. As a special case, we show the runtime of DGL with METIS partitions (denoted DGL-M) for papers on 32 hosts to discuss the differences with METIS. Partitioning for BatchGNN occurs in a distributed manner when the graph is loaded while DGL partitioning happens offline on a large memory machine independent of the experimental machines for each rank count.

The Adam optimizer is used to update gradients. We use a 0.003 learning rate. Dropout percentage for the GraphSAGE and GCN layers is 0.5. Sampling is with replacement for both training and testing. We drop the last training minibatch because that minibatch may contain a different number of vertices on each rank since it is not guaranteed that every rank has the exact same number of training vertices. PyTorch Distributed Data Parallel is used in both BatchGNN and DistDGL to synchronize gradients.

F Additional Experimental Results and Analysis

F.1 Full Set of Results

Table A1 and Table A2 show the full set of scaling results for the SAGE, GCN, and GIN experiments in the main paper. Specifically, it includes scaling for up to 32 ranks and the forward/backward breakdown for GCN and GIN both of which aren’t in the main paper due to space constraints. 1 rank papers100M is not included due to memory constraints. Speedup numbers in the main paper use the entirety of these numbers for their computation and not just the ones in Table 4.

Table A3 shows the aggregation cache initialization time. This is a one time cost that can be amortized over multiple epochs, and the cost decreases as the number of ranks increases due to additional compute power.

F.2 Discussion on Load Imbalance

What follows is an unabridged discussion with detailed experimental results on load imbalance that provides more detail than the main paper. Portions of this text are found in the main paper.

Observe in Table A1 and Table A2 that (1) DGL’s backward phase time for SAGE and GCN and (2) DGL’s forward phase time for GIN are both significantly higher than BGNN’s for some configurations (e.g., products and papers past 4 ranks): the reason for this is very heavy load imbalance in execution.

Table A4 illustrates load imbalance by showing the average difference between the fastest and slowest rank when it comes to subgraph preparation and forward phase time. This quantity is important because it is a measure of how long the entire system may be bottlenecked if there is a barrier during execution as all ranks would have to wait for the slowest rank. The backward phase for all models has a logical barrier due to the synchronization of weight gradients. Therefore, with high imbalance, the backward phase time recorded in the experiments will grow due to wait time.

We can explain the reason for DGL’s performance with this information. For products and papers past 4 ranks, the imbalance among ranks gets close or even surpasses the average prep and forward

Table A1: Average runtime (seconds) among all ranks and breakdown of distributed GNN training for 1 epoch for SAGE. Prep time includes time to prepare a subgraph: topology sampling, feature fetching, and export.

Graph	Ranks	System	SAGE						
			Subgraph Prep			Compute		Epoch	
			Topo	Feat	Export	Total	Fwd	Bwd	Total
arxiv	1	DGL	2.57	0.23	-	2.80	0.99	1.02	4.96
		BGNN	0.08	0.13	0.13	0.39	1.58	1.35	3.45
		BGNNC	0.07	0.11	0.06	0.29	1.70	1.43	3.53
	2	DGL	1.57	0.66	-	2.23	0.46	0.68	3.45
		BGNN	0.12	0.10	0.07	0.30	0.83	0.87	2.06
		BGNNC	0.09	0.06	0.04	0.21	0.59	0.75	1.61
	4	DGL	0.76	0.33	-	1.10	0.25	0.48	1.87
		BGNN	0.11	0.10	0.04	0.26	0.32	0.58	1.19
		BGNNC	0.11	0.07	0.03	0.22	0.34	0.44	1.03
products	1	DGL	16.93	2.29	-	19.22	5.00	4.71	29.22
		BGNN	0.64	1.18	1.46	3.37	5.52	4.88	14.04
		BGNNC	0.41	0.54	0.63	1.68	4.71	4.07	10.71
	2	DGL	11.74	10.10	-	21.84	2.90	4.04	28.92
		BGNN	0.83	1.00	0.91	2.79	2.86	2.33	8.11
		BGNNC	0.71	0.52	0.36	1.64	2.38	2.34	6.49
	4	DGL	5.89	4.24	-	10.13	1.60	3.67	15.47
		BGNN	0.52	0.87	0.46	1.89	1.41	1.54	4.90
		BGNNC	0.62	0.50	0.22	1.36	1.19	1.25	3.87
	8	DGL	3.21	4.48	-	7.70	0.84	3.30	11.88
		BGNN	0.45	0.73	0.31	1.52	0.71	0.86	3.12
		BGNNC	0.65	0.44	0.14	1.25	0.61	0.86	2.74
papers	2	DGL	73.00	77.41	-	150.41	17.71	24.51	193.96
		BGNN	3.98	18.74	6.10	29.13	16.27	17.51	63.86
		BGNNC	5.33	4.41	2.28	12.33	13.28	15.51	42.16
	4	DGL	34.27	31.06	-	65.32	8.74	18.49	93.09
		BGNN	2.35	7.20	3.78	13.64	8.69	10.75	33.61
		BGNNC	4.06	2.73	1.19	8.14	6.49	8.46	23.62
	8	DGL	19.24	38.00	-	57.24	4.52	39.85	101.91
		BGNN	1.37	5.64	1.61	8.73	3.96	6.77	19.70
		BGNNC	3.28	2.26	0.56	6.18	3.21	4.14	13.77
	16	DGL	10.01	26.57	-	36.58	2.17	28.13	67.03
		BGNN	0.76	4.38	0.88	6.09	1.96	3.34	11.50
		BGNNC	2.02	1.48	0.31	3.86	1.71	2.69	8.39
	32	DGL	5.64	21.49	-	27.13	1.08	13.66	41.96
		DGL-M	4.51	12.55	-	17.06	0.94	16.93	35.02
		BGNN	0.55	2.76	0.45	3.79	0.99	1.81	6.64
		BGNNC	1.41	1.06	0.15	2.65	0.86	2.17	5.73

Table A2: Average runtime (seconds) among all ranks and breakdown of distributed GNN training for 1 epoch for GCN and GIN. Prep time for these is similar to SAGE since the GNN layer differences will not change how sampling occurs. It can be derived by subtracting the forward and backward times from the epoch total.

Graph	Ranks	System	GCN			GIN		
			Compute		Epoch	Compute		Epoch
			Fwd	Bwd	Total	Fwd	Bwd	Total
arxiv	1	DGL	1.16	0.73	4.95	1.11	1.42	5.78
		BGNN	0.84	0.75	2.02	1.20	1.42	3.12
		BGNNC	1.05	0.93	2.28	1.38	1.62	3.41
	2	DGL	0.52	0.61	3.35	0.76	0.80	4.27
		BGNN	0.52	0.57	1.43	0.68	0.90	1.99
		BGNNC	0.56	0.75	1.58	0.83	1.05	2.26
	4	DGL	0.30	0.46	1.93	0.40	0.51	2.06
		BGNN	0.31	0.47	1.04	0.35	0.51	1.13
		BGNNC	0.29	0.38	0.90	0.36	0.53	1.15
products	1	DGL	7.76	4.24	31.57	5.15	7.24	31.80
		BGNN	5.00	3.25	12.11	7.08	8.31	19.05
		BGNNC	4.66	4.39	11.00	6.77	8.68	17.51
	2	DGL	3.74	2.72	27.23	3.48	4.27	28.67
		BGNN	2.68	2.29	7.77	3.67	4.68	11.31
		BGNNC	2.27	1.96	5.93	3.32	4.51	9.67
	4	DGL	2.05	2.87	15.84	2.54	2.36	15.37
		BGNN	1.32	1.46	4.72	1.87	2.51	6.59
		BGNNC	1.05	1.04	3.54	1.72	2.45	5.63
	8	DGL	1.05	6.30	16.07	5.31	1.51	15.15
		BGNN	0.64	0.73	2.84	0.96	1.44	3.86
		BGNNC	0.55	0.74	2.54	0.88	1.33	3.40
papers	2	DGL	22.29	21.63	190.62	21.54	23.86	188.11
		BGNN	17.29	18.53	64.67	23.76	32.78	89.22
		BGNNC	11.96	13.80	38.85	17.65	23.96	55.21
	4	DGL	11.07	15.73	93.61	18.17	13.33	99.93
		BGNN	7.93	11.31	32.89	11.40	20.29	45.51
		BGNNC	5.71	7.30	21.58	9.43	13.59	31.68
	8	DGL	5.65	39.09	100.61	37.85	7.28	100.68
		BGNN	3.46	5.83	18.00	4.77	7.38	20.97
		BGNNC	2.86	3.84	13.06	4.59	7.97	18.82
	16	DGL	2.84	29.73	71.52	29.44	4.27	71.89
		BGNN	1.77	2.93	11.09	2.58	3.82	12.54
		BGNNC	1.48	2.74	7.98	2.31	3.72	10.17
	32	DGL	1.43	14.87	42.96	13.67	2.29	43.33
		DGL-M	1.18	17.08	33.88	16.88	2.13	35.52
		BGNN	0.89	2.20	7.00	1.35	2.34	7.57
BGNNC		0.76	1.94	5.36	1.18	1.95	5.77	

Table A3: Aggregation cache initialization time (in seconds) for various graphs for the SAGE run.

	Ranks					
	1	2	4	8	16	32
arxiv	0.44	0.24	0.15	-	-	-
products	22.65	11.20	5.86	3.45	-	-
papers	-	320.69	176.11	87.95	45.69	23.22

Table A4: Average subgraph preparation and forward phase time (P+F) and the average difference (Rng.) in P+F between the fastest and slowest rank *for one minibatch* in an epoch for various graphs, rank (Rk.), and model configurations.

Graph	Rk.	Sys.	SAGE		GCN		GIN	
			P+F	Rng.	P+F	Rng.	P+F	Rng.
arxiv	2	DGL	0.06	0.01	0.06	0.01	0.08	0.00
		BGNN	0.03	0.00	0.02	0.00	0.02	0.00
	4	DGL	0.06	0.01	0.07	0.02	0.07	0.00
		BGNN	0.03	0.01	0.02	0.01	0.03	0.00
product	2	DGL	0.26	0.02	0.25	0.01	0.25	0.00
		BGNN	0.06	0.00	0.06	0.01	0.07	0.00
	4	DGL	0.24	0.07	0.27	0.07	0.27	0.01
		BGNN	0.07	0.01	0.07	0.01	0.08	0.01
	8	DGL	0.36	0.22	0.41	0.40	0.57	0.01
		BGNN	0.09	0.01	0.09	0.01	0.10	0.01
paper	2	DGL	0.29	0.02	0.29	0.03	0.28	0.00
		BGNN	0.08	0.01	0.08	0.02	0.09	0.01
	4	DGL	0.25	0.07	0.26	0.07	0.29	0.00
		BGNN	0.08	0.02	0.07	0.02	0.08	0.02
	8	DGL	0.42	0.42	0.42	0.41	0.63	0.01
		BGNN	0.09	0.02	0.08	0.02	0.09	0.01
	16	DGL	0.53	0.57	0.57	0.63	0.92	0.01
		BGNN	0.11	0.03	0.11	0.02	0.12	0.01
	32	DGL	0.78	0.63	0.78	0.66	1.14	0.01
		BGNN	0.50	0.75	0.46	0.73	0.92	0.01

pass time. This indicates heavy imbalance that results in the high backward phase time shown in Table A1 and Table A2 for SAGE and GCN. For GIN, the forward phase time is instead very high for DGL compared to BGNN, and the imbalance shown in Table A4 is actually low. The reason for this is also imbalance: Torch Distributed Data Parallel (DDP, the mechanism used to synchronize models in our experiments) adds a barrier before the *forward* phase in GIN (Our testing suggests that DDP inserts this barrier if there are many learnable parameters in the model. GIN has more parameters to learn than SAGE and GCN.), so the imbalance present in the sampling and feature fetching (the main source of imbalance in these runs) causes all ranks to wait for the straggler host before forward rather than at backward. The result is that the imbalance for prep and forward phase is low due to the existence of the barrier, but the imbalance overhead is now reflected in GIN’s very high time in Table A2. The reason that DGL-M does not result in a larger performance improvement over DGL can be explained with imbalance as well. METIS partitions result in more relative imbalance than random partitions as shown in Table A4, so the backward time for SAGE/GCN and forward time in GIN in Table A1 and Table A2 for DGL-M is higher than that of normal DGL.

BatchGNN does not have these issues: Table A4 shows all configurations are relatively balanced. Any sampling imbalance only occurs when fetching macrobatches rather than for every minibatch in the macrobatch. Macrobatching *mitigates* the effect of imbalance because sampling does not occur past the first minibatch of a macrobatch. When minibatches are sampled one at a time like in DGL, sampling imbalance reoccurs for every minibatch, *amplifying* the imbalance. Therefore, a major takeaway is that macrobatching improves runtime by mitigating load imbalance overheads.

G Links to Used Resources

The OGBN datasets can be found here: <https://ogb.stanford.edu/docs/nodeprop/>

DGL code can be found here: <https://github.com/dmlc/dgl>

LDBC can be found here: <https://ldbcouncil.org/benchmarks/snb/>

The MKL package we used is 2022.1.0, hc2b9512_224, and can be found here: <https://anaconda.org/anaconda/mkl/files>